Robotics and Autonomous Systems 10 (1992) 209–224
Elsevier

Singularity analysis and representation of planar parallel manipulators

Jaouad Sefrioui and Clément M. Gosselin

Dépt. de Génie Mécanique, Université Laval, Ste-Foy, Québec, Canada, G1K 7P4

Communicated by F.C.A. Groen

Abstract

Sefrioui, J. and Gosselin, C.M., Singularity analysis and representation of planar parallel manipulators, Robotics and Autonomous Systems, 10 (1992) 209–224.

In this paper, analytical expressions describing the singularity loci of simple planar three-degree-of-freedom parallel manipulators are derived. They are obtained using the analytical form of the Jacobian matrix, which is known to be singular when the manipulator is in a degenerate configuration. The expressions derived are then used to superimpose graphical representations of the manipulators' singularity loci and workspace. Both types of local degeneracies that can occur for parallel manipulators are studied. However, architecture singularities, which are rather trivial for the type of manipulators studied here, are assumed to be avoided by a proper choice of the manipulator's kinematic parameters. It is shown that, given certain assumptions on the geometry and for a given orientation of the end-effector, the singularity locus in the (x, y) plane will always be a hyperbola. Moreover, when the passive revolute joints on the base and on the platform are respectively placed symmetrically, the hyperbola degenerates into a straight line. All these results are illustrated with examples of planar parallel manipulators. Some cases for which the singularities are located outside of the workspace are also presented. The analytic description of the singularity loci of manipulators in the Cartesian space can be used for analysis and optimum kinematic design. The expressions derived here have been integrated in a CAD package for parallel manipulators which provides a quick graphical representation of the singularity loci.

Keywords: Parallel manipulator; Singularity; Degeneracy; Singularity locus; Jacobian matrix; Direct kinematic problem; Inverse kinematic problem; Workspace; Computer aided design; Graphical simulation.

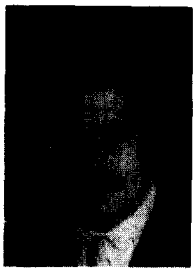

Jaouad Sefrioui received the B.Sc. and the M.Sc. in Physics from the Université Mohammed *V*, Rabat, Morocco, in 1981, and the Doctorate degree in Physics from the Université de Dijon, Dijon, France, in 1984. From 1984–1989 he was an Assistant Professor of mechanics in the Department of Physics, Université Ibno-Tofaïl, Kenitra, Morocco. Since May 1990, he has been a Ph.D. candidate in the Department of Mechanical Engineering, Université Laval, Ste-Foy, Québec, Canada, under the supervision of Professor Clément Gosselin. His current research interests are the kinematics and the dynamics of parallel robotic manipulators.

Clément M. Gosselin received the B. Eng. degree in mechanical engineering from the Université de Sheerbrooke, Québec, Canada, in 1985, and the PhD. degree in mechanical engineering from McGill University, Montréal, Québec, Canada, in 1988. He received the D.W. Ambridge award from McGill for the best thesis of the year in Physical Sciences and Engineering. In 1988–89, he spent one year as a postdoctorate student in INRIA (Institut National de Recherche en Informatique et en Automatique) in Sophia-Antipolis, France, where he worked within the PRISME (Programmation des Robots Industriels et des Systèmes Manipulateurs Evolués) research team. Since June 1989, he has been an Associate Professor in the Department of Mechanical Engineering, Université Laval, Ste-Foy, Québec, Canada. His research interests are kinematics, dynamics and control of robotic mechanical systems with a particular emphasis on the mechanics of grasping and on the kinematics and dynamics of parallel manipulators. Dr. Gosselin is a member of ASME and IEEE.

1. Introduction

The optimum kinematic design of manipulators has attracted the attention of researchers for some years. More specifically, most of the work that has been done on the subject has been directed towards the optimization of dexterity or manipulability indices which are known to be related to the kinematic accuracy [3,7,11,18,23]. In the context of parallel manipulators, kinematic accuracy is a very important issue. Indeed, it is well known that a special type of local degeneracy can occur in the motion of these manipulators. This type of singularity is termed *singularity of type II* in [4]. Physically, these configurations lead to: (i) an instantaneous change in the degree-of-freedom of the system and hence a loss of the controllability, and (ii) an important degradation of the natural stiffness which may lead to very high joint forces or torques. Therefore, it is very important to be able to identify singular configurations at the design stage in order to improve the system's performance.

The singularities of serial manipulators have been studied by several researchers (see for instance [1,8,9,12,13,19,22]). Some researchers have also considered closed kinematic chains [2,14,15,20]. In [4], it has been shown that, by writing the velocity equations of closed chains in terms of two Jacobian matrices, it is possible to classify the singularities in three different types which have different physical interpretations. In [16], Merlet used Grassmann geometry to study the singularities of spatial six-degree-of-freedom parallel manipulators. He obtained an exhaustive list of possible singular configurations. The latter method is general and can be applied to various mechanisms with any degree of freedom.

However, in the context of design, it is desirable to develop a tool that will allow to determine easily the locus of singular configurations in the manipulator's Cartesian workspace. In other words, given a set of design parameters, provide the designer with a representation of the singularity locus. Such a result cannot be achieved with geometrical methods. The approach used here consists in obtaining analytical expressions for the determinant of the Jacobian matrix and in using them to construct the loci. In this paper, these expressions have been obtained for simple planar three-degree-of-freedom parallel manipulators. It is shown that the singularity locus is in fact a hyperbola in the Cartesian space for a given orientation of the platform. A graphical tool has been developed to provide an interactive representation of the singularity locus in the Cartesian space. The aim of this tool is to help the designer by allowing him to determine the exact locus of the singular configurations of a particular design and hence to be able to make decisions on whether or not the singularities encountered are acceptable. Cases for which the singularities are located outside of the workspace are shown.

2. Singularity analysis

Let $\boldsymbol{\theta}$ be the vector of actuated joint coordinates and $\boldsymbol{x}$ be the Cartesian coordinate vector of an n-degree-of-freedom parallel manipulator. We have

$$\boldsymbol{\theta} = [\theta_1, \theta_2, \ldots, \theta_n]^{\mathrm{T}}, \tag{1}$$

$$\boldsymbol{x} = [x_1, x_2, \ldots, x_n]^{\mathrm{T}}, \tag{2}$$

where θ_i represents either the angular rotation of a revolute joint or the linear displacement of a prismatic joint and x_i is a Cartesian coordinate, i.e., a component of a position or an orientation. We will also refer to vectors $\boldsymbol{\theta}$ and $\boldsymbol{x}$ as the input and output coordinates, respectively. These two vectors are related through a system of nonlinear algebraic equations representing the geometric constraints and which can be written as

$$\boldsymbol{F}(\boldsymbol{\theta}, \boldsymbol{x}) = \boldsymbol{0}, \tag{3}$$

where $\boldsymbol{0}$ is the n-dimensional zero vector. Differentiating Eq. (3) with respect to time will lead to

$$\boldsymbol{A}\dot{\boldsymbol{x}} + \boldsymbol{B}\dot{\boldsymbol{\theta}} = \boldsymbol{0}, \tag{4}$$

where $\boldsymbol{A}$ and $\boldsymbol{B}$ are square matrices of dimension n. These configuration dependent matrices are called Jacobian matrices.

Considering Eq. (4), three types of singularities, each of which having a differential physical interpretation, have been defined by Gosselin and Angeles [4]. These singularities occur, respectively, when (i) matrix $\boldsymbol{B}$ is rank-deficient, (ii) matrix $\boldsymbol{A}$ is rank-deficient or (iii) the positioning equations degenerate. As pointed out in [4], only the first type of singularity is possible for serial-type manipulators. The physical interpretation of

each of the three types of singularity is given in detail in the same reference. They are briefly repeated here for quick reference.

2.1. First type of singularity

Referring to Eq. (4), the first type of singularity will occur when we have

$$\det(\boldsymbol{B}) = 0. \tag{5}$$

The corresponding configurations are located at the boundary of the workspace of the manipulator or on internal boundaries between regions of the workspace in which the number of solutions of the inverse kinematic problem is different. Moreover, since the nullspace of $\boldsymbol{B}$ is not empty, there exist nonzero vectors $\dot{\boldsymbol{\theta}}$ which will correspond to a vanishing Cartesian velocity vector. In other words, some velocities cannot be produced at the end-effector. Moreover, in virtue of the kinematic–static duality [21], there exist wrenches that will not affect the actuators when applied to the end-effector.

2.2. Second type of singularity

Referring again to Eq. (4), the second type of singularity occurs when matrix $\boldsymbol{A}$ is rank-deficient, i.e.,

$$\det(\boldsymbol{A}) = 0. \tag{6}$$

As opposed to the first type of singularity, this type of degeneracy can occur inside the manipulator's Cartesian workspace and will correspond to the set of configurations for which two different branches of the direct kinematic problem meet. In fact, this is why this type of singularity cannot occur for serial manipulators since the direct kinematic problem always leads to a unique solution. From Eqs. (4) and (6) and since the nullspace of matrix $\boldsymbol{A}$ is not empty, there exist nonzero Cartesian velocity vectors $\dot{\boldsymbol{x}}$ which will be mapped into a vanishing actuator velocity vector. The corresponding configuration will be one in which an infinitesimal motion of the end-effector is possible even if the actuators are locked. In other words, the end-effector gains one or several degrees of freedom and the manipulator's stiffness vanishes in some directions.

2.3. Third type of singularity

This type of singularity is of a slightly different nature than the first two. It corresponds to a degeneracy of the *positioning* or *orientation* equations. Some conditions on the geometric parameters of the robot are required for this type of singularity to occur. Indeed, only certain special architectures will lead to this type of singularity which justifies the term *architecture singularity* used in [15] to designate them.

Such singularities will lead to configurations where a finite motion of the end-effector is possible even if the actuators are locked or in situations where a finite motion of the actuators produces no motion of the end-effector. In both cases, the manipulator cannot be controlled.

The classification presented above is general and can be applied to any closed-loop mechanism (examples of the application of the method to simple mechanisms can be found in [4]). In this paper, we will study the loci of the first two types of singularities for planar three-degree-of-freedom parallel manipulators. We will assume that the architecture singularities are avoided by a proper choice of the kinematic parameters. In fact, the geometric conditions under which such manipulators will exhibit singularities of the third type are given in [4] and can easily be avoided.

3. Planar three-degree-of-freedom parallel manipulators

In this section, the singularity loci of some planar three-degree-of-freedom parallel manipulators will be determined. The manipulators considered here are actuated with prismatic joints and are such that the passive revolute joints on the platform are aligned. This is represented in *Fig. 1*. A particular case for which the base and the platform are symmetric will also be studied. The kinematics of this type of manipulator has been studied extensively in [3] and [17].

3.1. Planar three-degree-of-freedom parallel manipulators with a colinear platform

A manipulator of this type is shown in *Fig. 1*. Now, let $\boldsymbol{x} = [x, y, \phi]^{\mathrm{T}}$ be the vector of Cartesian coordinates of the manipulator, representing

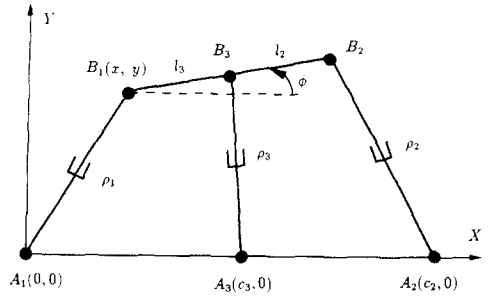

Fig. 1. Planar three-degree-of-freedom parallel manipulator with aligned joints on the base and on the platform.

the position of one point on the platform and the orientation of the platform. Moreover, let $\boldsymbol{\theta} = [\rho_1, \rho_2, \rho_3]^T$ be the vector of joint coordinates, representing the length of each of the legs of the manipulator. The inverse kinematics is then easily written as:

$$\rho_1^2 = x^2 + y^2, \tag{7}$$

$$\rho_2^2 = (x + l_2 \cos\phi - c_2)^2 + (y + l_2 \sin\phi)^2, \tag{8}$$

$$\rho_3^2 = (x + l_3 \cos\phi - c_3)^2 + (y + l_3 \sin\phi)^2, \tag{9}$$

where l_2, l_3, c_2 and c_3 are defined in *Fig. 1*, i.e., $l_2 = \overline{B_1B_2}$, $l_3 = \overline{B_1B_3}$, $c_2 = \overline{A_1A_2}$ and $c_3 = \overline{A_1A_3}$.

Differentiating Eqs. (7)–(9) with respect to time leads to:

$$\boldsymbol{A}\dot{\boldsymbol{x}} + \boldsymbol{B}\dot{\boldsymbol{\theta}} = 0,$$

where $\boldsymbol{A}$ and $\boldsymbol{B}$ are the two Jacobian matrices, which can be expressed as

$$\boldsymbol{A} = \begin{bmatrix} x & y & 0 \\ (x - c_2) + l_2 \cos\phi & y + l_2 \sin\phi & l_2[y \cos\phi - (x - c_2)\sin\phi] \\ (x - c_3) + l_3 \cos\phi & y + l_3 \sin\phi & l_3[y \cos\phi - (x - c_3)\sin\phi] \end{bmatrix}. \tag{10}$$

$$\boldsymbol{B} = \mathrm{diag}[\rho_1, \rho_2, \rho_3]. \tag{11}$$

3.1.1. Singularities of type I

These singularities occur when

$$\det(\boldsymbol{B}) = 0. \tag{12}$$

Mathematically, this condition will lead to

$$\rho_1 = 0 \quad \text{or} \quad \rho_2 = 0 \quad \text{or} \quad \rho_3 = 0.$$

However, since the actuators do not have an infinite range of motion, this type of singularity will in fact occur when one of the actuators reaches one of its limits, i.e.,

$$\rho_i = \rho_{i,\min} \quad \text{or} \quad \rho_i = \rho_{i,\max}, \quad i = 1, 2, \text{or } 3. \tag{13}$$

The locus of these singularities is simply the limits of the Cartesian workspace and can be easily obtained [6].

3.1.2. Singularities of type II

A singular configuration of type II occurs when

$$\det(\boldsymbol{A}) = 0.$$

From Eq. (10), the determinant of matrix $\boldsymbol{A}$ can be written as

$$\det(\boldsymbol{A}) = A_1 y^2 + A_2 xy + A_3 y + A_4 x, \tag{14}$$

where the coefficients, A_i, $i = 1, 2, 3, 4$, are functions of the orientation of the platform and of the kinematic parameters of the robot. They are given as

$$A_1 = -(c_3 l_2 - c_2 l_3)\cos\phi, \tag{15}$$

$$A_2 = (c_3 l_2 - c_2 l_3)\sin\phi, \tag{16}$$

$$A_3 = \sin\phi[(c_2 - c_3) l_2 l_3 \cos\phi - c_2 c_3 (l_2 - l_3)], \tag{17}$$

$$A_4 = -(c_2 - c_3) l_2 l_3 \sin^2\phi. \tag{18}$$

Therefore, the locus of the singular configurations of type II in the Cartesian space, for a given orientation of the platform, are the set of points which satisfy the following condition:

$$A_1 y^2 + A_2 xy + A_3 y + A_4 x = 0, \tag{19}$$

which is an algebraic equation of degree 2. The nature of this curve, in the XY plane, will depend on the sign of Δ [10], a quantity defined as

$$\Delta = -\frac{A_2^2}{4}.$$

Since Δ is negative definite, the singularity locus, as defined in Eq. (19), will be a hyperbola [10]. The properties of the hyperbola will depend on the orientation of the platform and on the kinematic parameters of the robot. These properties are very important since they will affect the kinematic behavior of the robot. For instance, the location of the hyperbola in the workspace of the manipulator can be very critical. In fact, we would like, if possible, to move away the hyperbola from the workspace of the manipulator. In order to derive conditions under which such results can be obtained, the hyperbola of Eq. (19) will be studied in the next section. Of particular interest will be the minimum distance between the two branches of the hyperbola.

3.1.3. Geometric study of the hyperbola

From Eq. (19), the two different branches of the hyperbola can be obtained, i.e.,

$$y_1 = \frac{1}{2}\left[-\frac{A_3 + A_2 x}{A_1} + \sqrt{\frac{-4A_4 x}{A_1} + \frac{(A_3 + A_2 x)^2}{A_1^2}} \right], \quad (20)$$

$$y_2 = \frac{1}{2}\left[-\frac{A_3 + A_2 x}{A_1} - \sqrt{\frac{-4A_4 x}{A_1} + \frac{(A_3 + A_2 x)^2}{A_1^2}} \right]. \quad (21)$$

(a) Equations of the asymptotes: The equations of the branches of the hyperbola presented above lead to the following asymptotes:

$$y = -\frac{A_4}{A_2}, \quad (22)$$

$$y = \frac{-(A_2 A_3) + A_1 A_4}{A_1 A_2} + px, \quad (23)$$

where

$p = \tan \phi$

is the slope of the oblique asymptote. The hyperbolas obtained with four different values of ϕ are represented in *Fig. 2*, for a given manipulator.

It can be noticed that the two asymptotes given by Eqs. (22) and (23) become identical when $\phi = \pi/2$ or $\phi = 3\pi/2$. In this case, the hyperbola degenerates into a straight line. A three-dimensional representation of the type II singularity locus is given in *Fig. 3*. The upper branch of the hyperbola is represented in *Fig. 3a*, while the lower branch is shown in *Fig. 3b*.

(b) Evolution of the center point of the hyperbola: The intersection of the two asymptotes of the hyperbola is referred to as the center of the hyperbola. If we denote the coordinates of this point by (x_0, y_0), we can write:

$$x_0 = B_2 + B_1 \cos \phi, \quad (24)$$

$$y_0 = B_1 \sin \phi, \quad (25)$$

with

$$B_1 = \frac{(c_2 - c_3) l_2 l_3}{c_3 l_2 - c_2 l_3}, \quad (26)$$

$$B_2 = \frac{c_2 c_3 (l_2 - l_3)}{c_3 l_2 - c_2 l_3}. \quad (27)$$

From Eqs. (24) and (25) and from the following trigonometric identity,

$\cos^2 \phi + \sin^2 \phi = 1,$

the curve described by the center of the hyperbola when angle ϕ is incremented can be obtained as:

$$y_0^2 + (x_0 - B_2)^2 = B_1^2. \quad (28)$$

Clearly, the curve obtained is a circle of radius B_1 in the XY plane, whose center is given by $(B_2, 0)$. The direction of the progression of the center of the hyperbola around the circle depends on the sign of B_1, which in turn depends on the kinematic parameters of the robot. For the example mentioned above, B_1 is positive and therefore the center of the hyperbola will move counterclockwise when ϕ is increased.

(c) Minimum distance between the two branches of the hyperbola: An interesting property of the singularity locus is the minimum distance between the two branches of the hyperbola, referred to as distance AB in *Fig. 2a*. The computation of this distance is simplified when the axes of symmetry of the hyperbola are used as a working coordinate frame. In order to do this, a translation of the origin of the reference frame to point (x_0, y_0) is first performed. Then, a rotation of angle α around this point is performed, so that both set of axes coincide. The details are given in the Appendix. The computation of the distance AB leads to a few different cases, depending on the geometry of the manipulator and on the orientation ϕ. Indeed, the equation of the hyperbola, expressed in a coordinate frame formed by its axes of symmetry can be written as (see Appendix):

$$\frac{Y^2}{H_{0y}} - \frac{X^2}{H_{0x}} = 1, \quad (29)$$

with

$$H_{0x} = \frac{2c_2c_3l_2l_3(c_3 - c_2)(l_2 - l_3)\sin^2\phi}{(c_3l_2 - c_2l_3)^2(1 - \cos\phi)},$$

$$H_{0y} = \frac{2c_2c_3l_2l_3(c_3 - c_2)(l_2 - l_3)\sin^2\phi}{(c_3l_2 - c_2l_3)^2(1 + \cos\phi)}. \quad (30)$$

It is shown in the Appendix that H_{0x} and H_{0y} are always of the same sign, thereby proving that Eq. (29) represents a hyperbola.

The minimum distance between the two branches, AB, depends on the signs of H_{0x} and H_{0y}. The latter depends solely on the sign of a product of two quantities. These quantities are function of the geometry of the robot only and are given by:

$$(c_3 - c_2)(l_2 - l_3).$$

This leads to a few different cases which are summarized in *Table 1*.

The minimum distance between the two branches of the hyperbola, distance AB, will now be plotted as a function of the orientation of the platform, for a given geometry. Two examples, corresponding to the two classes of manipulators presented in *Table 1* are studied.

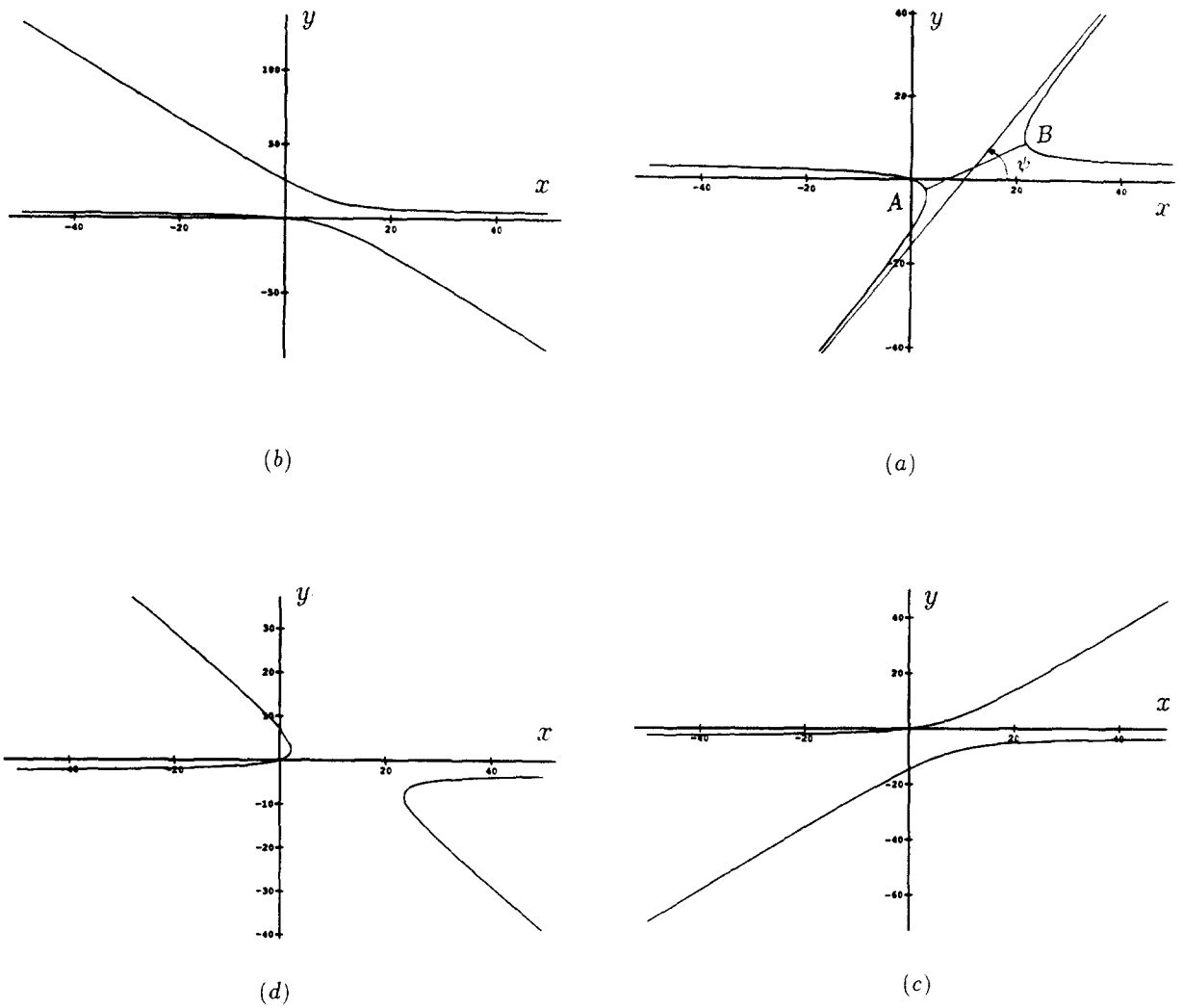

Fig. 2. Singularity locus of a planar three-degree-of-freedom manipulator with $l_2 = 4$, $l_3 = 1$, $c_2 = 3$ and $c_3 = 5$, for (a) $\phi = 1$ rad, (b) $\phi = 2$ rad, (c) $\phi = 4$ rad and (d) $\phi = 5.5$ rad.

Example 1: $c_2 = 5$, $c_3 = 2$, $l_2 = 4$ and $l_3 = 1$. For this architecture, we have:

$$(c_3 - c_2)(l_2 - l_3) < 0.$$

The minimum distance between the branches of the hyperbola is represented in *Fig. 4a* as a function of angle ϕ, i.e., the orientation of the platform. This distance is found to be relatively large for values of angle ϕ within the range bounded by $-\pi/2$ and $\pi/2$. Moreover, the distance is maximum when angle ϕ is close to 0.

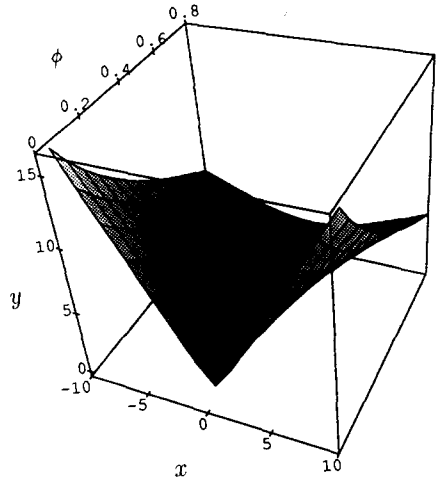

(*a*)

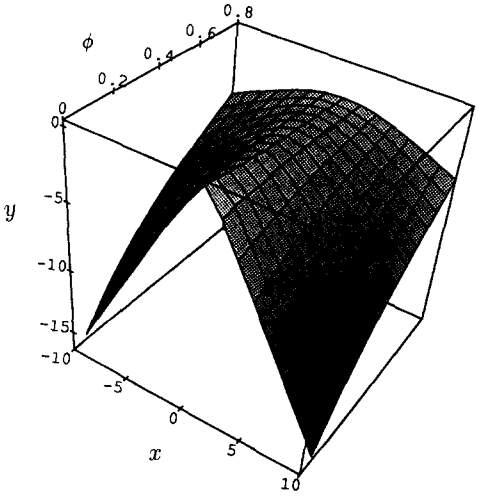

(*b*)

Fig. 3. Three-dimensional representation of the type *II* singularity locus.

Table 1
Formulae for the computation of the minimum distance between the branches of the hyperbola

$\text{sgn}[(c_3 - c_2)(l_2 - l_3)]$	$\text{sgn}[H_{0x}$ or $H_{0y}]$	AB
> 0	> 0	$2\sqrt{H_{0y}}$
< 0	< 0	$2\sqrt{-H_{0x}}$

Example 2: $c_2 = 5$, $c_3 = 2$, $l_2 = 1$ and $l_3 = 4$. In this case, we have:

$$(c_3 - c_2)(l_2 - l_3) > 0.$$

Fig. 4b shows that the minimum distance between the branches is maximum when angle ϕ is close to π and that this distance is relatively large when ϕ is comprised between $\pi/2$ and $3\pi/2$.

3.1.4. Singularity loci and workspace

Another interesting issue in this study is the location of the singularity loci with respect to the actual workspace of the manipulator. Indeed, part of the singularity locus – or even the entire locus – may be located outside of the workspace of the manipulator. In this paragraph, we will superimpose the singularity curves described above and the limits of the workspace of the manipulator which have been obtained from the algorithm presented in [5] and [6]. The graphical representation of this superposition was performed by a simulation software (SIMPA) developed at Laval [6]. Some results are represented on *Figs. 5* and *6*, respectively, for the two examples of manipulators treated above. In these figures, the limit of the workspace is represented by a solid curve. Hence, this curve is at the same time the locus of the singularities of type I. Actuator ranges comprised between 2.5 and 7.5 units of length have been used in order to simulate a very good mobility of the legs. The locus of the singularities of type II is represented by the dotted curve, which is of course a hyperbola. It is noted that for some values of angle ϕ – the orientation of the platform – the singularities of the second type are located outside of the workspace. This type of analysis is therefore of great interest for the design of parallel manipulators since singularities can be easily predicted.

3.2. Simplified symmetric planar parallel manipulators

A particular class of planar three-degree-of-freedom parallel manipulators will now be studied. This class is composed of manipulators whose base and platform are symmetric with respect to the central passive revolute joint, i.e., the manipulators for which

$$c_2 = 2c_3. \tag{31}$$

$$l_2 = 2l_3. \tag{32}$$

For this class of manipulators, the singularities of

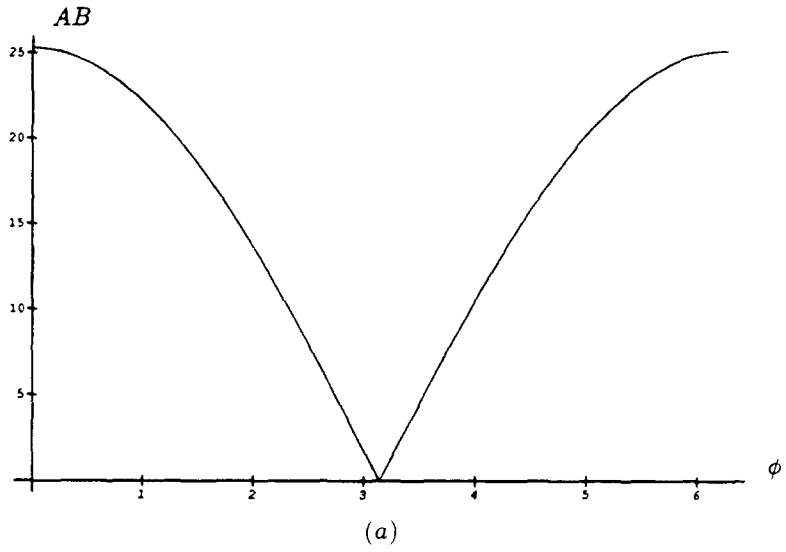

(a)

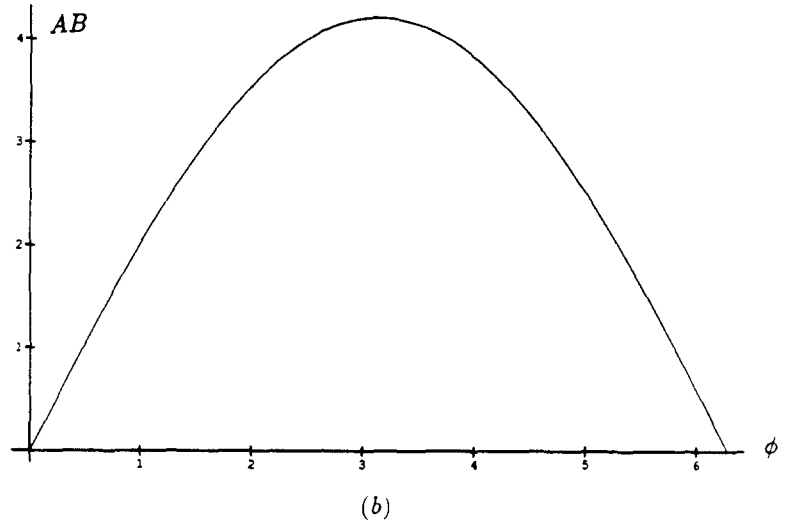

(b)

Fig. 4. The minimum distance between the two branches of the hyperbola as a function of the orientation of the platform ϕ.

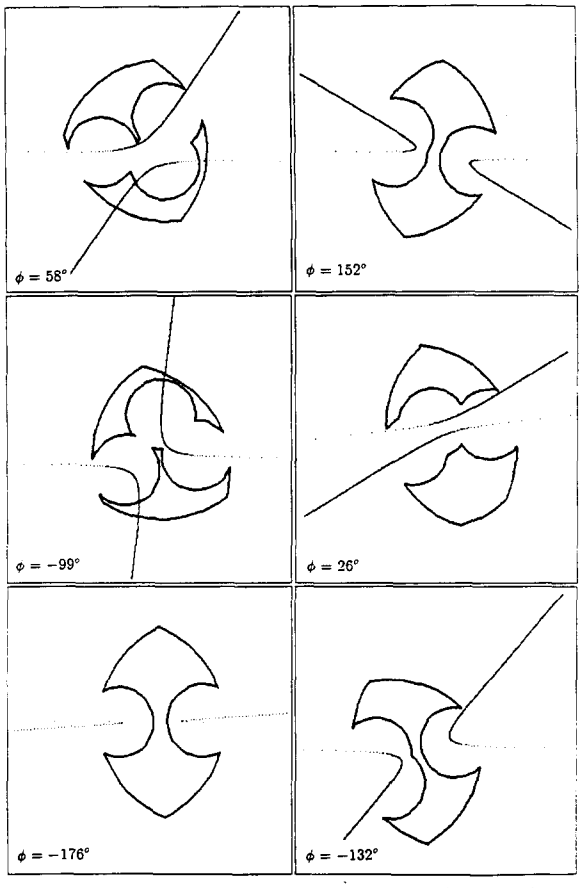

Fig. 5. Superposition of the workspace and the Singularity locus of a planar 3-dof manipulator with $l_2 = 4$, $l_3 = 1$, $c_2 = 5$ and $c_3 = 2$.

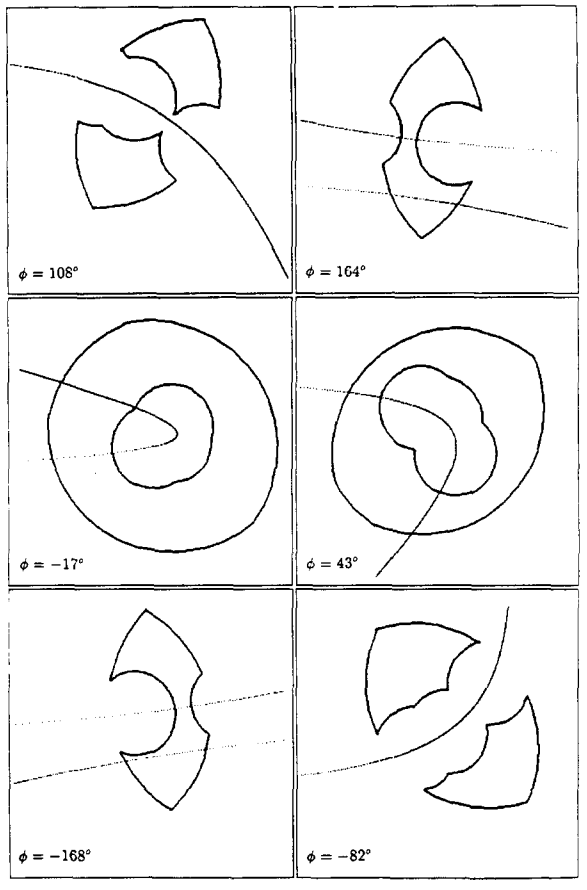

Fig. 6. Superposition of the workspace and the Singularity locus of a planar 3-dof parallel manipulator with $l_2 = 1$, $l_3 = 4$, $c_2 = 5$ and $c_3 = 2$.

type *I* are, again, described by condition (13). However, Eq. (19), describing the singularities of type *II*, is simplified by the intoduction of Eqs. (31) and (32). The conditions for a singularity of type *II* then become:

$$\sin \phi = 0 \Rightarrow \phi = k\pi, \quad k = 0, \pm 1, \ldots, \tag{33}$$

or

$$y(c_3 - l_3 \cos \phi) + x(l_3 \sin \phi) = 0,$$
$$\phi \neq k\pi, \quad k = 0, \pm 1, \ldots \tag{34}$$

For a given value of ϕ such that $\phi \neq k\pi$ and $\cos \phi \neq c_3/l_3$, Eq. (34) is the equation of a straight line passing through the origin of the coordinates, i.e.,

$$y = -\frac{l_3 \sin \phi}{c_3 - l_3 \cos \phi} x. \tag{35}$$

The physical interpretation of these conditions is now examined. In fact, it can be shown that these conditions are verified if and only if the lines associated with each of the three legs of the manipulator have a common point of intersection.

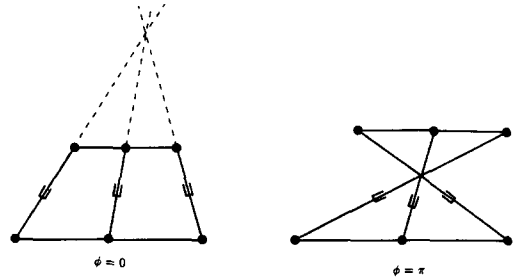

Fig. 7. The two singularities of type *II* associated with $\sin \phi = 0$.

Let x_1, x_2 and x_3 be three variables associated with the lines comprising segments $\overline{A_1B_1}$, $\overline{A_2B_2}$ and $\overline{A_3B_3}$, respectively. The corresponding equations can be written as:

$$xy_1 - yx_1 = 0. \tag{36}$$

$$(-c_3 + x + l_3 \cos\phi)y_2 - (y + l_3 \sin\phi)x_2 + c_3(y + l_3 \sin\phi) = 0. \tag{37}$$

$$(-2c_3 + x + 2l_3 \cos\phi)y_3 - (y + 2l_3 \sin\phi)x_3 + 2c_3(y + 2l_3 \sin\phi) = 0. \tag{38}$$

These lines have a common intersection if and only if the determinant associated with the above system of equations vanishes, i.e.,

$$\sin\phi[y(c_3 - l_3 \cos\phi) + x(l_3 \sin\phi)] = 0, \tag{39}$$

which is equivalent to Eqs. (33) and (34). Hence,

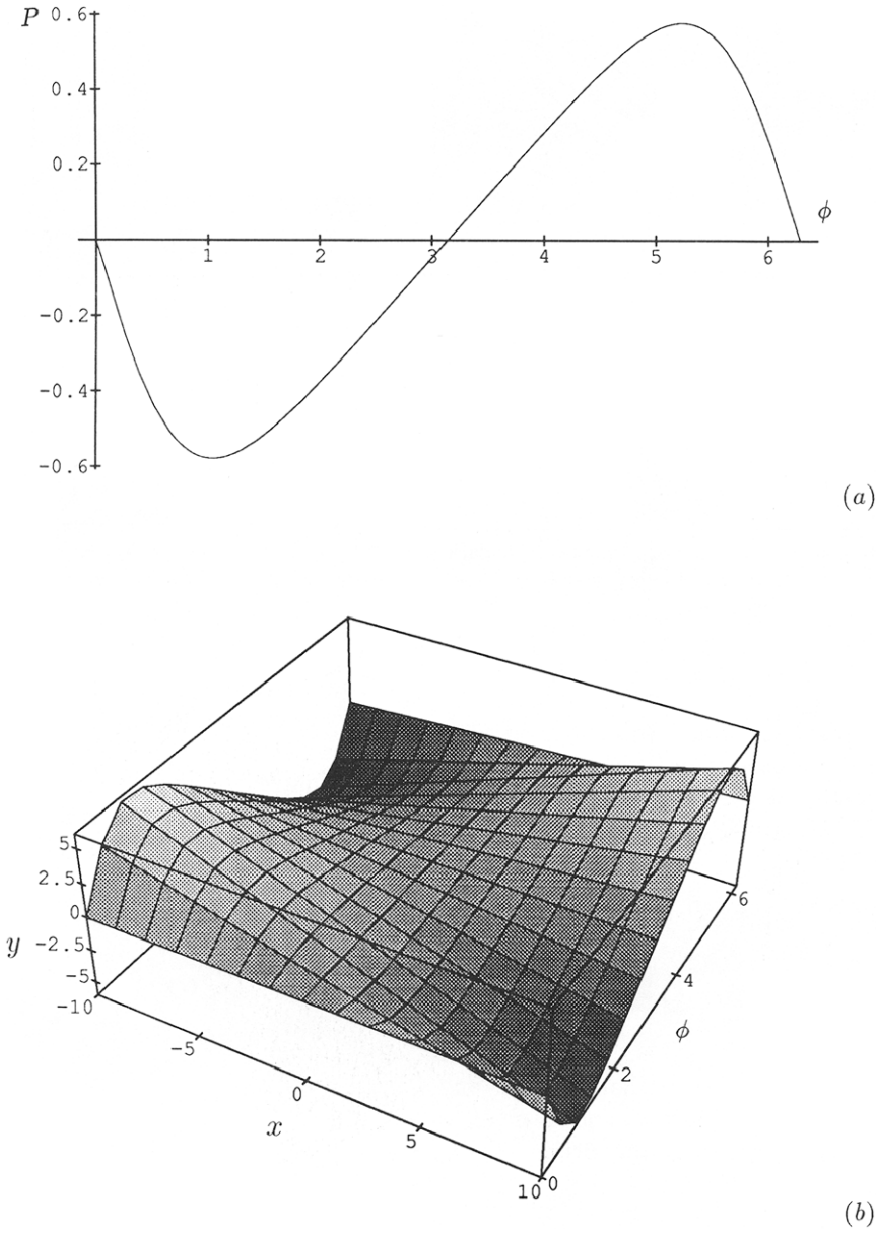

Fig. 8. (a) Slope of the singularity line, and (b) singularity locus for $c_3 = 2$ and $l_3 = 1$.

simplified symmetric planar parallel three-degree-of-freedom manipulators have a singularity of type *II* if the lines along the three legs have a common intersection. This result is in agreement with the results obtained in [16] using Grassmann geometry. Two different cases are identified:

Case 1: Eq. (33) shows that when $\sin \phi = 0$, the simplified symmetric manipulator is in a singular configuration, whatever its particular geometry is. The two different cases for which this situation can occur are represented in *Fig. 7*.

Case 2: For values of ϕ such that

$$\phi \neq k\pi \quad \text{and} \quad \cos \phi \neq \frac{c_3}{l_3}$$

singularities of type *II* are represented by Eq.

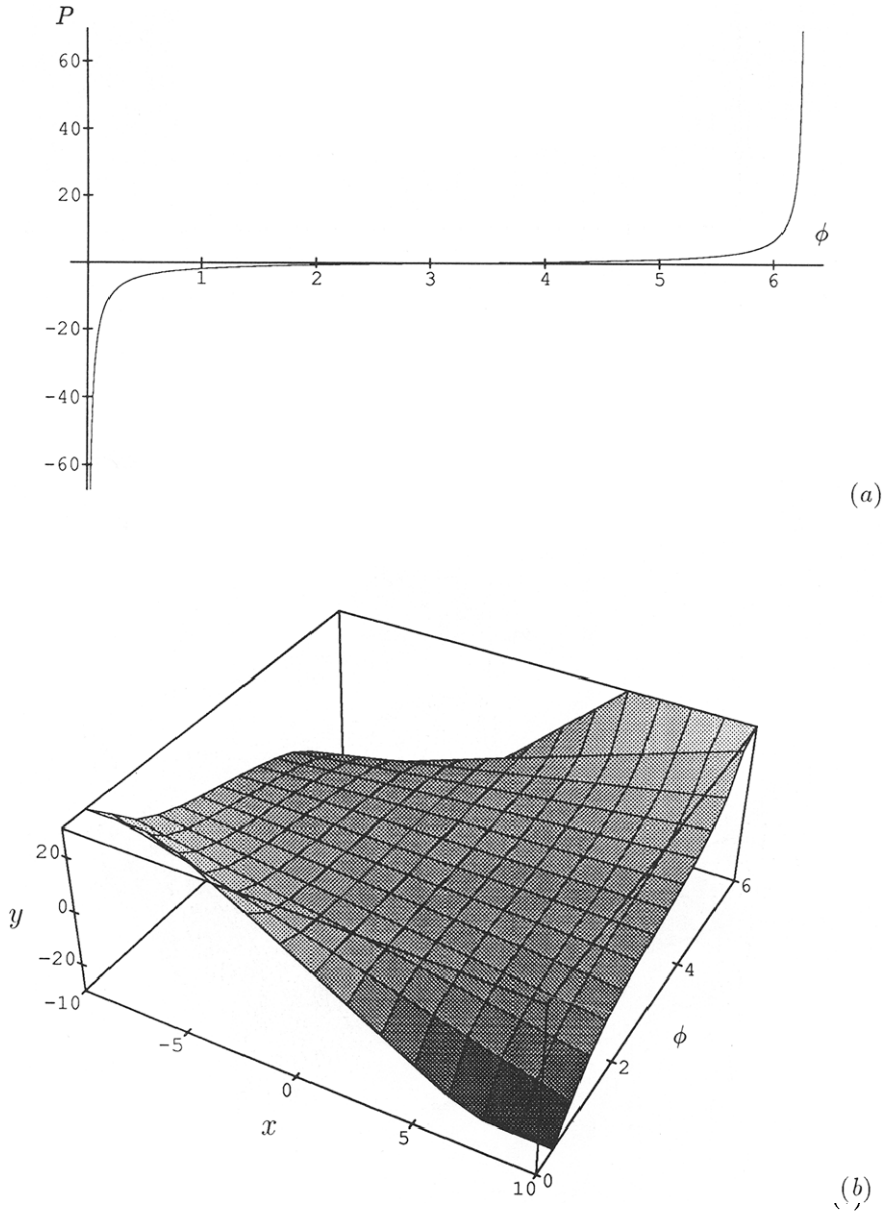

Fig. 9. (a) Slope of the singularity line, and (b) singularity locus for $c_3 = l_3$.

(35). For each value of angle ϕ, there will exist a singularity line passing through the origin. The slope of this line is given by:

$$p = -\frac{l_3 \sin \phi}{c_3 - l_3 \cos \phi}. \quad (40)$$

It is pointed out that, for a given geometry of the manipulator, the slope p of the straight line describing the singularity locus – Eq. (40) – depends on angle ϕ only. A plot of p as a function of ϕ as well as a three-dimensional representation of the corresponding singularity locus has been obtained for the three following cases:

$$c_3 > l_3,\ c_3 = l_3, \quad \text{and} \quad c_3 < l_3.$$

The respective plots and singularity loci, which are ruled surfaces, are given in *Figs. 8, 9* and *10*.

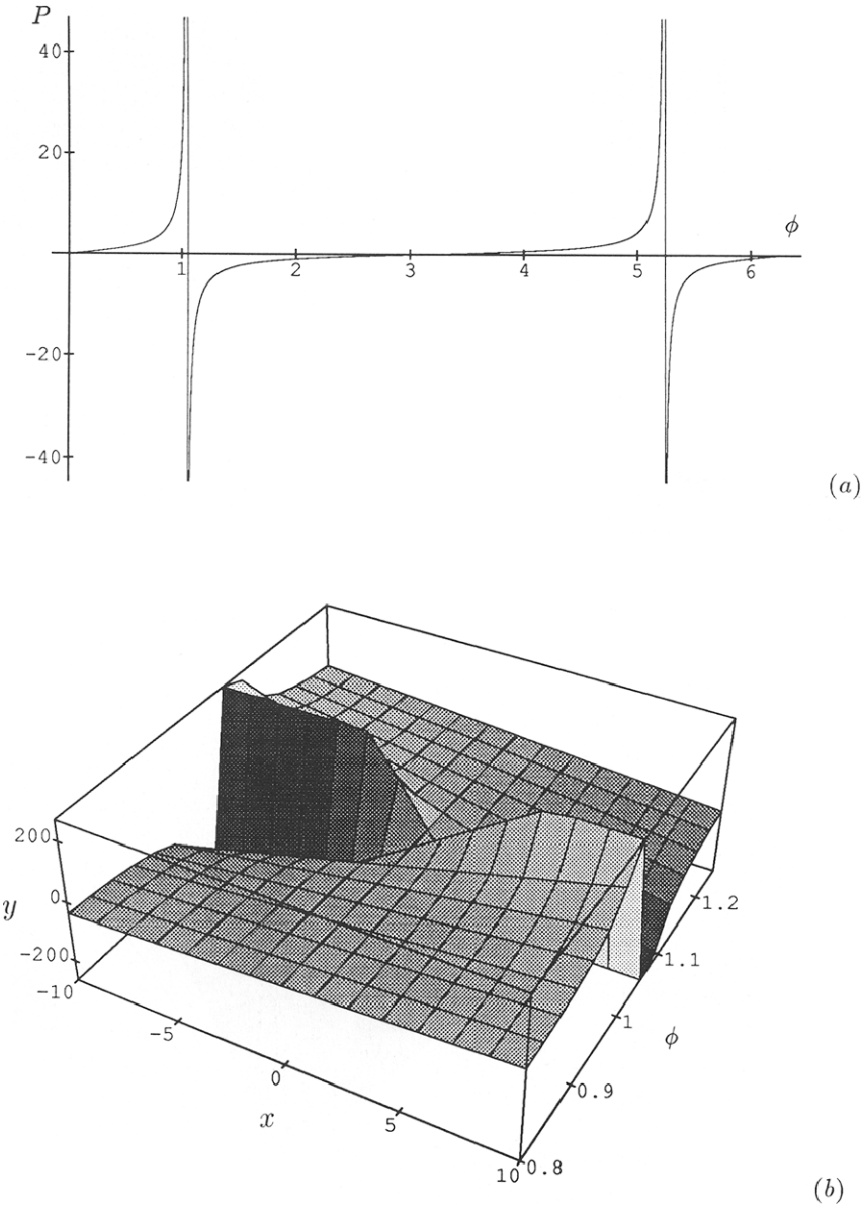

Fig. 10. (a) Slope of the singularity line, and (b) singularity locus for $c_3 = 1$ and $l_3 = 2$.

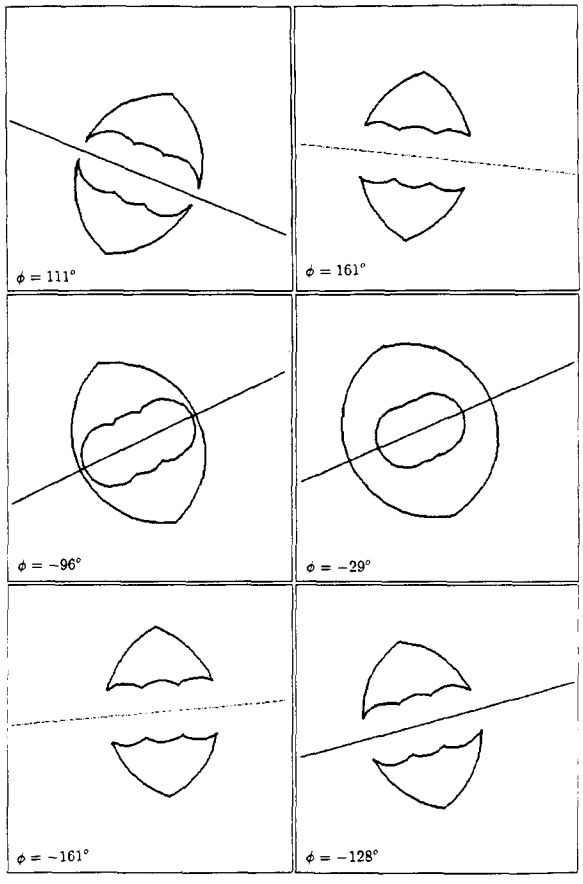

Fig. 11. Superposition of the workspace and the Singularity locus of a simplified planar 3-dof parallel manipulator with $l_2 = 2$, $l_3 = 1$, $c_2 = 4$ and $c_3 = 2$.

3.2.1. Singularity loci and workspace

Again, for this particular case of planar parallel manipulator, the singularity loci are superimposed on the workspace of the manipulator. This is represented in *Fig. 11* for given orientations of a simplified symmetric manipulator having the following dimensions:

$$c_2 = 4,\ c_3 = 2,\ l_2 = 2, \quad \text{and} \quad l_3 = 1.$$

The workspace of this manipulator has been defined using limit values of 2.5 and 7.5 units for the length of each of the legs. We have assumed a large range of values of the ρ_i's in order to allow the platform to reach virtually all possible orientations.

The singularities of type *I* correspond to the limit of the workspace and are represented as solid curves. On the other hand, singularities of type *II* are represented as dotted curves. Again, it appears clearly that, for some orientations of the platform, the type *II* singularity curve is located outside of the workspace of the manipulator. In other words, for these orientations of the platform, the manipulator cannot be in a singular configuration of type *II*.

4. Conclusion

The analytical determination and the graphical representation of the singularity loci of planar three-degree-of-freedom parallel manipulators with prismatic actuators has been presented in this paper. The method used here is based on the derivation of an explicit expression for the determinant of the Jacobian matrix of the manipulator. This expression is then used to obtain a graphical representation of the singularity loci, for singularities of type *II*. On the other hand, as expected, the singularities of type *I* correspond to the limits of the Cartesian workspace.

For parallel manipulators whose unactuated revolute joints on the platform are aligned, it has been shown that the singularities of type *II* lead to a locus described by a hyperbola which degenerates into a straight line for some specific orientations. A three-dimensional representation of this locus has also been presented. Moreover, it has been shown that the center of the hyperbola moves along a circle when angle ϕ – describing the orientation of the platform – is incremented. The center and the radius of this circle are functions of the geometric parameters of the manipulator. The singularity locus and the Cartesian workspace have then been superimposed. Simulations have shown that with certain geometric parameters and for certain orientations of the platform, the singularities are located outside of the workspace.

A particular class of symmetric manipulators has been studied. In this case, singularities of type *II* occur whenever the platform is oriented horizontally, i.e., whenever ($\phi = k\pi$, $k = 0, \pm 1, \ldots$). This result is applicable to all symmetric manipulators regardless of the geometric parameters. This type of architecture is therefore ill-conditioned *a priori*. Additionally, if ($\phi \neq k\pi$, $k = 0, \pm 1, \ldots$), then the singularity locus is a straight line. The slope of this line depends on the geometric parameters of the manipulator and on the

orientation of the platform. A three-dimensional representation of the singularity locus obtained in this case has been presented. Again, for some geometric parameters of the manipulator and for some orientations of the platform, the singularity locus can be located outside of the workspace.

The analytical expressions developed here for the singularity loci are of great interest for the design of parallel manipulators. They have been implemented in a computer simulator which allows the designer to visualize interactively the singularity locus superimposed on the workspace.

5. Appendix: Computation of the minimum distance between two branches of a hyperbola

Let the equation of the hyperbola be written as:

$$A_1 y^2 + A_2 xy + A_3 y + A_4 x = 0, \tag{41}$$

with

$$A_1 = -(c_3 l_2 - c_2 l_3)\cos\phi,$$

$$A_2 = (c_3 l_2 - c_2 l_3)\sin\phi,$$

$$A_3 = \sin\phi[(c_2 - c_3) l_2 l_3 \cos\phi - c_2 c_3 (l_2 - l_3)],$$

$$A_4 = -(c_2 - c_3) l_2 l_3 \sin^2\phi.$$

The two branches of the hyperbola can be identified as,

$$y_1 = \frac{1}{2}\left[-\frac{A_3 + A_2 x}{A_1} + \sqrt{\frac{-4A_4 x}{A_1} + \frac{(A_3 + A_2 x)^2}{A_1^2}}\right],$$

$$y_2 = \frac{1}{2}\left[-\frac{A_3 + A_2 x}{A_1} - \sqrt{\frac{-4A_4 x}{A_1} + \frac{(A_3 + A_2 x)^2}{A_1^2}}\right],$$

and the equations of the asymptotes are written as:

$$y = -\frac{A_4}{A_2},$$

$$y = \frac{-(A_2 A_3) + A_1 A_4}{A_1 A_2} - \frac{A_2 x}{A_1}.$$

The center of the hyperbola is then obtained as,

$$x_0 = \frac{-(A_2 A_3) + 2A_1 A_4}{A_2^2},$$

$$y_0 = -\frac{A_4}{A_2},$$

i.e.,

$$x_0 = \frac{c_2 c_3 l_2 - c_2 c_3 l_3 + c_2 l_2 l_3 \cos\phi - c_3 l_2 l_3 \cos\phi}{c_3 l_2 - c_2 l_3},$$

$$y_0 = \frac{(c_2 - c_3) l_2 l_3 \sin\phi}{c_3 l_2 - c_2 l_3},$$

where

$$x_0 = B_2 + B_1 \cos\phi,$$

$$y_0 = B_1 \sin\phi,$$

and

$$B_1 = \frac{(c_2 - c_3) l_2 l_3}{c_3 l_2 - c_2 l_3},$$

$$B_2 = \frac{c_2 c_3 (l_2 - l_3)}{c_3 l_2 - c_2 l_3}.$$

Change of origin: The origin of the coordinate frame is first moved to point (x_0, y_0), the center of the hyperbola. We have:

$$x' = x - x_0.$$

$$y' = y - y_0.$$

Eq. (41) can then be written as

$$-A_2 A_3 A_4 + A_1 A_4^2 + A_2^3 x' y' + A_1 A_2^2 y'^2 = 0, \tag{42}$$

with

$$A_2 \neq 0$$

Rotation of the coordinates: The new coordinate frame is then rotated through an angle η, i.e.,

$$x' = X \cos \eta - Y \sin \eta,$$

$$y' = X \sin \eta + Y \cos \eta,$$

where angle η is defined as

$$\eta = \frac{\psi}{2} = \frac{\phi}{2},$$

(c.f. *Fig. 2a*) where ψ is the angle between the non-horizontal asymptote, whose slope is given by p, and the X axis. Hence,

$$p = \tan \psi = -A_2/A_1 = \tan \phi, \tag{43}$$

and the equation of the hyperbola in the new reference frame (X, Y) can be written as:

$$-(A_2A_3A_4) + A_1A_4^2 + A_2^3XY \cos^2\eta + A_1A_2^2Y^2 \cos^2\eta,$$

$$+A_2^3X^2 \cos \eta \sin \eta + 2A_1A_2^2XY \cos \eta \sin \eta,$$

$$-A_2^3Y^2 \cos \eta \sin \eta + A_1A_2^2X^2 \sin^2\eta - A_2^3XY \sin^2\eta = 0. \tag{44}$$

The following trigonometric transformations are then applied to Eq. (44):

$$\cos^2\frac{\psi}{2} + \sin^2\frac{\psi}{2} = 1,$$

$$\cos \frac{\psi}{2} \sin \frac{\psi}{2} = \frac{\sin \psi}{2},$$

$$\sin^2\frac{\psi}{2} = \frac{1 - \cos \psi}{2},$$

$$\sin \psi = -\frac{A_2 \cos \phi}{A_1},$$

with

$$\tan \theta = p = -A_2/A_1 = \tan \phi.$$

Eq. (44) then becomes

$$H_0 + H_xX^2 - H_yY^2 = 0, \tag{45}$$

where

$$H_0 = 2A_1A_4(-(A_2A_3) + A_1A_4),$$

$$H_x = A_2^2(-A_2^2 \cos \phi + A_1^2(1 - \cos \phi)),$$

$$H_y = -A_2^2(A_2^2 \cos \phi + A_1^2(1 + \cos \phi)),$$

i.e.,

$$H_0 = -2c_2(c_2 - c_3)c_3l_2(l_2 - l_3)l_3(c_3l_2 - c_2l_3) \times (-(c_3l_2) + c_2l3) \cos \phi \sin^4\phi$$

$$H_x = -(c_3l_2 - c_2l_3)^4(1 - \cos \phi) \cos \phi \sin^2\phi$$

$$H_y = -(c_3l_2 - c_2l_3)^4(1 + \cos \phi) \cos \phi \sin^2 \phi$$

We now assume that: $c_2 \neq c_3$, $l_2 \neq l_3$, $c_3l_2 \neq c_2l_3$, $\cos \phi \neq 0$ and $\sin \phi \neq 0$. It is then possible to divide Eq. (45) by H_0, which leads to:

$$1 - Y^2/H_{0y} + X^2/H_{0x} = 0, \tag{46}$$

where

$$H_{0y} = \frac{H_0}{H_y},$$

$$H_{0x} = \frac{H_0}{H_x},$$

i.e.,

$$H_{0x} = \frac{2c_2c_3l_2l_3(c_3 - c_2)(l_2 - l_3) \sin^2\phi}{(c_3l_2 - c_2l_3)^2(1 - \cos \phi)}$$

$$H_{0y} = \frac{2c_2c_3l_2l_3(c_3 - c_2)(l_2 - l_3) \sin^2\phi}{(c_3l_2 - c_2l_3)^2(1 + \cos \phi)}$$

The nature of the curve of Eq. (46) depends on the sign of H_{0x} and H_{0y} or, in other words, of the sign of H_x and H_y.

Let us now consider the sign of the product H_xH_y:

$$H_xH_y = (c3l2 - c2l3)^8 \sin^6\phi \cos^2\phi > 0,$$

hence, H_{0x} and H_{0y} will always have the same sign, which again shows that Eq. (46) represents a hyperbola.

The minimum distance between the two branches of the hyperbola can then be computed. Two different cases arise depending if H_{0x} and H_{0y} are both positive or negative. The sign of H_{0x} and H_{0y} depends on the sign of:

$$(c_3 - c_2)(l_2 - l_3).$$

Acknowledgements

This work was completed under research grants from the Natural Sciences and Engineering Re-

search Council of Canada (NSERC) and le Fonds pour la Formation des Chercheurs et l'Aide à la Recherche (FCAR) of Québec. The authors also wish to acknowledge the help of Simon Laverdière who wrote and implemented the software allowing the graphical representation of the singularity loci.

References

[1] J. Angeles, K. Anderson, X. Cyril and B. Chen, The kinematic inversion of robot manipulators in the presence of singularities, *ASME Journal of Dynamic Systems, Measurement, and Control* 110 (1988) 246–254.

[2] J.E. Baker, Screw system algebra applied to special linkage configurations, *Mechanism and Machine Theory* 15 (4) (1980) 255–256.

[3] C.M. Gosselin and J. Angeles, The optimum kinematic design of a planar three-degree-of-freedom parallel manipulator, *ASME Journal of Mechanisms, Transmissions and Automation in Design* 110 (1) (1988) 35–41.

[4] C.M. Gosselin and J. Angeles, Singularity analysis of closed-loop kinematic chains, *IEEE Transactions on Robotics and Automation* 6 (3) (1990) 281–290.

[5] C.M. Gosselin, Determination of the worspace of 6-DOF parallel manipulators, *ASME Journal of Mechanical Design* 112 (3) (1990) 331–336.

[6] C.M. Gosselin, S. Laverdière and J. Côté, SIMPA: A graphic simulator for the CAD of parallel manipulators, *Proc. of the ASME Computers in Engineering Conference*, Vol. 1, San Francisco (1992) 465–471.

[7] C.M. Gosselin and J. Angeles, A global performance index for the kinematic optimization of robotic manipulators, *ASME Journal of Mechanical Design* 113 (3) (1991) 220–226.

[8] K.H. Hunt, Special configurations of robot-arms via screw theory, Part 1: The Jacobian and its matrix cofactors, *Robotica* 4 (1986) 171–179.

[9] K.H. Hunt, Special configurations of robot-arms via screw theory, Part 2: Available end-effector displacements, *Robotica* 5 (1987) 17–22.

[10] A.C. Jones, *Introduction to Algebraical Geometry* (Oxford University Press, Oxford, 1912).

[11] C.A. Klein and B.E. Blaho, Dexterity measures for the design and control of kinematically redundant manipulators, *The International Journal of Robotics Research* 6 (2) (1987) 72–83.

[12] Z.C. Lai and D.C.H. Yang, A new method for the singularity analysis of simple six link manipulators, *The International Journal of Robotics Research* 5 (2) (1986) 66–74.

[13] F.L. Litvin, Y. Zhang, V. Parenti-Castelli and C. Innocenti, Singularities, configurations, and displacement functions for manipulators, *The International Journal of Robotics Research* 5 (2) (1986) 52–65.

[14] F.L. Litvin, J. Tan, P. Fanghella and S. Wu, Singularities in motion and displacement fonctions for the RCRCR, RCRRC and RSRC linkage, Part 1: Basic concepts, *Proc. 13th ASME Design Automation Conference*, Boston (1987) 267–278.

[15] O. Ma and J. Angeles, Architecture singularities of platform manipulators, *Proc. IEEE International Conference on Robotics and Automation*, Sacramento, CA (1991) 1542–1547.

[16] J.P. Merlet, Singular configurations of parallel manipulators and Grassmann geometry, *The International Journal of Robotics Research* 8 (5) (1989) 45–56.

[17] J.P. Merlet, Les robots parallèles, *Traité des nouvelles Technologies, Série Robotique* (Hermes, France, 1990).

[18] J.K. Salisbury and J.J. Craig, Articulated hands: Force control and kinematic issues, *The International Journal of Robotics Research* 1 (1) (1982) 4–17.

[19] T. Shamir, The singularities of redundant robot arms, *The International Journal of Robotics Research* 9 (1) (1990) 113–121.

[20] K. Sujimoto and J. Duffy, Application of linear algebra to screw systems, *Mechanism and Machine Theory* 17 (1) (1982) 73–83.

[21] K.J. Waldron and K.H. Hunt, Series-parallel dualities in actively coordinated mechanisms, in R. Bolles and B. Roth, eds., *Robotics Research* 4 (1988) 175–181.

[22] S.L. Wang and K.J. Waldron, A study of singular configurations of serial manipulators, *ASME Journal of Mechanisms, Transmissions and Automation in Design* 109 (1) (1987) 14–20.

[23] T. Yoshikawa, Manipulability of robotic mechanisms, *The International Journal of Robotics Research* 4 (2) (1985) 3–9.